האגוד הישראלי למכניקה עיונית ושימושית

The Israel Society for Theoretical and Applied Mechanics

ISTAM

An Adhering Organization of the
International Union of Theoretical and Applied Mechanics
(IUTAM: http://www.iutam.net)

ISTAM Annual Symposium

TECHNICAL PROGRAM

17 December 2006

Tel Aviv University

ISTAM Annual Symposium

17 December 2006

TECHNICAL PROGRAM

Location: Rosenblatt Auditorium, Computer and Software Engineering Building,Tel Aviv University

09:30 – 09:50 Registration and coffee

09:50 – 10:00 *Opening:* M.B. Rubin, Technion, President of ISTAM

Morning Session Chairman: **D. Durban**, Technion

10:00 – 10:25 M. Mata, O. Casals, D. Esqué, N. Cuadrado and **J. Alcalá**, Universitat Politècnica de Catalunya. *Contact deformation regimes in sharp and spherical indentation experiments: mechanical property extractions*

10:25 – 10:50 **Y. Benveniste**, Tel Aviv University. *A general interface model for a three-dimensional curved thin interphase*

10:50 – 11:15 **S. Vigdergauz**, The Israel Electric Corporation. *Energy-minimizing inclusion in an elastic plate under remote shear*

11:15 – 11:40 **E. Zaretsky**, B. Herrmann, and D. Shvarts. Ben Gurion University. *Dynamic strength of uranium at high temperatures*

Graduate Research Lecture Session Chairman: **R. Masri**, Technion

11:40 – 11:50 **E. Chesla** and D. Durban, Technion. *Large strain response of uniformly stressed elastoplastic solids under superposed simple shear*

11:50 – 12:00 **D. Shaine**, L. Tevet-Deree and G. deBotton. Ben-Gurion University. *Electroactive polymer composites – coupled electro-mechanical FE*

12:00 – 12:10 **A. Ovcharenko**, G. Halperin and I. Etsion, Technion. *Experimental investigation of contact area during normal loading-unloading in elastic-plastic spherical contact using direct optical technique*

12:10 – 12:20 **V. Brizmer**, Y. Kligerman and I. Etsion, Technion. *Elastic-Plastic Spherical Contact under Combined Normal and Tangential Loading*

12:20 – 12:30 **Y. Kadin**, Y. Kligerman and I. Etsion, Technion. *Yielding inception of adhesive micro-contact*

12:30 – 14:00 Lunch (The registration fee includes lunch)

Afternoon Session Chairman: **G. deBotton**, Ben-Gurion University

14:00 – 14:25 **I. Blechman**. Technion. *Relaxation and pure creep under new paradigm*

14:25 – 14:50 **M. Perl** and J. Perry, Ben Gurion University. *A numerical model for evaluating the residual stress field in an autofrettaged spherical pressure vessel incorporating the Bauschinger effect*

14:50 – 15:15 **A. Wolf**, Technion. *Open mechanics problems in Biomechanics and Robotics*

15:15 – 15:40 **R. De**, A. Zemel and S.A. Safran. Weizmann Institute of Science. *Dynamics of Cell Orientation*

15:40 – 16:05 **M. Jabareen** and M.B. Rubin. Technion. *A generalized 3-D brick Cosserat point element for nonlinear elasticity: Comparison with other element formulation*

The annual membership fee to ISTAM is 50 NIS. It includes the lunch at the symposium and can be paid during the registration.

All lectures are open to the public free of charge

Contact deformation regimes in sharp and spherical indentation experiments: mechanical property extractions

M. Mata, O. Casals, D. Esqué, N. Cuadrado and J. Alcalá*

Department of Materials Science and Engineering
ETSEI Barcelona, Universitat Politècnica de Catalunya
Avda. Diagonal 647, 08028 Barcelona, Spain
*Lecturer: Email: jorge.alcala@upc.es

Indentation experiments have long been employed in the assessment of the mechanical behavior of materials and structures at small length scales. An important issue in the analysis of these experiments involves extraction of the uniaxial mechanical properties of the indented solid. This requires knowledge of the relationships existing between the contact parameters and the uniaxial stress-strain curve, which is grounded in the field of contact mechanics. This presentation covers some of the work performed by the authors on the influence of plastic deformation and strain hardening upon the contact response. This issue is examined in detail by recourse to extensive finite element simulations of conical, pyramidal (Vickers and Berkovich) and spherical indenters in solids obeying the J_2 associated-flow plasticity theory.

First, a review is given on the contact deformation regimes attained in sharp indentation experiments. Along these lines, it is shown that the development of plastic flow is amenable to analysis through the concept of the characteristic stress, which was originally introduced by Tabor, regardless of whether the solid behaves within the elasto-plastic or the fully plastic regimes. The analysis leads to a general relationship which correlates hardness with the yield strength, σ_{ys}, hardening exponent, n, and Young's modulus, E. The consideration of material pileup and sinking-in responses, in conjunction with the abovementioned correlation, leads to a general methodology for extracting the mechanical properties through conventional hardness tests. The analysis is extended to spherical (Brinell) indentation where, in this case, the evolution from the elasto-plastic to the fully plastic contact regimes is additionally controlled by length-scale imposed by the ratio between contact radius and indenter's diameter, a/D. The coupling of the finite element simulations to dimensional analysis of the contact problem provides a relationship between hardness, the mechanical properties and a/D. Such a general relationship accurately captures the evolution from the Hertzian (elastic) to the fully plastic regimes that occurs as a/D is increased, enabling mechanical property extractions from a series of hardness tests performed at different applied loads.

Attention is finally given to the analysis of instrumented indentation experiments, which allow one to measure the applied load (P)-penetration depth (h_s) curves during the loading and unloading stages of the experiment. Along these lines, new developments are presented showing that there are two sets of σ_{ys}, n and E that can be extracted from any given P-h_s curve. Such a fundamental duality in mechanical property extractions emerges essentially because in metallic materials, any unloading segment of a P-h_s curve can be accurately modeled with two different n values. It is found that simple experimental evaluations of the geometrical appearance of a Vickers or Berkovich imprint allow one to readily discern which of the two sets of properties truly pertains to the indented material. Experiments are performed in a number of metals showing that although the mechanical properties are extremely sensitive to slight changes in the P-h_s curves, the proposed methodology can still successfully evaluate the overall features of the uniaxial stress-strain curve of the material within a reasonable accuracy. The presentation ends with a brief discussion on the influence of crystal slip anisotropy upon the contact response. This is a relevant issue since most of the nano- and micro-indentation experiments are performed at load ranges where the imprint lies well within a single grain of micro-constituent.

Keywords: Contact mechanics, plasticity, nano-indentation, hardness.

References

[1] O. Casals and J. Alcalá, "The Duality in Mechanical Property Extractions from Vickers and Berkovich Instrumented Indentation Experiments", *Acta Materialia*, 53 3545-: 3561 (2005).

[2] M. Mata and J. Alcalá, "Mechanical Property Evaluation through Sharp Indentation in Elasto-plastic and Fully Plastic Contact Regimes" *Journal of Materials Research*, 18 1705-1709 (2003).

[3] M. Mata, M. Anglada and J. Alcalá, "Contact Deformation Regimes Around Sharp Indentations and the Concept of the Characteristic Strain", *Journal of Materials Research*, 17 964-976 (2002).

A general interface model for a three-dimensional curved thin interphase

Y. Benveniste

Department of Solid Mechanics, Materials and Systems,
Faculty of Engineering, Tel-Aviv University, Ramat-Aviv, Tel-Aviv, 69978 Israel
Email: benben@eng.tau.ac.il

The modelling of a thin interphase between two media by a so called "imperfect interface", on which certain appropriate interface conditions prevail, has been one of standing interest in the mechanics literature. Often, the described representation is convenient and simplifies the solution of boundary value problems involving the original three-phase configuration of an interphase between its neighbouring media. This lecture will report on the findings of recent works of the author on the subject [Benveniste (2006a,b), Benveniste and Baum (2006)].

In Bövik and Olsson (1992), and Bövik (1994), Taylor expansions of the relevant physical fields within the interphase were combined with the use of surface differential operators on a curved surface in order to achieve the representation of a thin isotropic interphase by an imperfect interface. The derived interface model in those works is of $O(h)$ accuracy where h denotes the thickness of the interphase. The ideas in these two studies were recently revisited and generalized by the present author. In Benveniste (2006a), an $O(h)$ interface model is derived for a generally curved anisotropic interphase between two anisotropic media in the setting of unsteady thermal conduction and dynamic elasticity. In Benveniste (2006b), an $O(h^N)$ interface model (with N being an arbitrary integer) is developed for an isotropic interphase between two isotropic solids in the setting of steady thermal conduction. The findings of that second paper are readily transferable to the analogous physical phenomena of electrical conduction, dielectrics, magnetism, diffusion, flow in porous media, and can in principle be extended to the more complex contexts of elasticity, coupled field effects, anisotropic constituents, and time dependent fields. In Benveniste and Baum (2006), the model has been extended to the case of graded interphases.

The derived interface model consists of expressions for the jumps in the displacements and tractions (temperature and normal heat flux in thermal conduction) across the interface. These jumps are expressed in terms of a hierarchy of surface differential forms which depend on the material properties of the neighbouring media and of the interphase that has been eliminated, and involve surface derivatives of the displacements and tractions (temperature and normal heat flux) along the interface. The formulated interface model is applicable for the whole flexibility (conductivity) spectrum of the interphase. Several well known imperfect interface models which are valid for soft or stiff (poorly conducting or highly conducting) interphases are recovered as special cases the presently derived model. The validity of the interface model is tested in the setting of a coated fiber embedded in an infinite medium which is subjected at infinity to a certain temperature loading, and the predictions of the $O(h), O(h^2)$ and $O(h^3)$ models are compared with those of the exact solution.

References

[1] Benveniste, Y. 2006a. A general interface model for a three-dimensional curved thin anisotropic interphase between two anisotropic media. *J. Mech. Phys Solids*, **54**, 708-734.

[2] Benveniste, Y. 2006b. An $O(h^N)$ interface model of a three-dimensional curved interphase in conduction phenomena. *Proc. Roy. Soc London A*, **462,** 1593-1617.

[3] Benveniste, Y. and Baum, G. 2006. An interface model of a graded three-dimensional anisotropic curved interphase. *Proc. Roy. Soc London A*, in press.

[4] Bövik, P. and Olsson, P. 1992. Effective boundary conditions for the scattering of two-dimensional SH waves from a curved thin elastic layer. *Proc. Roy. Soc London A* **439**, 257-269.

[5] Bövik, P. 1994. On the modelling of thin interface layers in elastic and acoustic scattering problems. *Q. J. Mech. Appl. Math*. **47**, 17-42.

Energy-minimizing inclusion in an elastic plate under remote shear

S. Vigdergauz

Research and Development Division, The Israel Electric Corporation Ltd., P.O.Box 10,
Haifa 31000, Israel. Email: smuel@iec.co.il

Elastostatic analysis and optimization of fibre-reinforced composites is a topic of current interest in different fields of structural engineering. An important problem here is to shape a fixed volume of the fibres in such a way as to minimize the strain energy increment induced in a given homogeneous stress state of the matrix and hence to maximize the structure overall rigidity.

Like in other branches of continuum mechanics, the stress-strain analysis of bi-material structures is being developed to a far greater extent than the optimization of their mechanical properties, even in a linear case. The reason is that closed-form optima are extremely rare, whereas numerical schemes involve a computationally hard repetitive solving of the fourth-order elasticity equations in a successively modified region. The resulted chain of forward boundary-value problems becomes especially severe in a multi-connected domain when a reinforcing phase is arranged into a set of interacting inclusions.

The alternative optimization strategy offers to obtain the exact geometrically independent lower bounds on the strain energy in terms of the phases elastic moduli and their relative volumes. The bounds attainability is proved directly through the explicit identification of the extremal structures. The bound-saturating phases arrangement appears to be different for bulk and pure shear trial loadings. The bulk global minimum is attained at several structures including a matrix with the specifically shaped (equi-stress) inclusions. By contrast, the shear global minimum is associated with only the technologically unavailable multi-scale laminates.

By this reason, we consider here the energy minimization problem for a narrowed set of more credible composites formed by a single foreign fibre perfectly embedded in an infinite matrix. This model presents a dilute limit for multi-fibre materials with vanishingly small interaction. Though simple in concept, this scheme is very hard computationally. For further simplicity, we consider the shapes conformally mapped onto a circle by an analytic function with only one non-zero Laurent term. This one-parameter shape optimization with an integral objective functional is then solved using an enhanced complex-variable approach. The obtained results give the energy minimum and the corresponding Laurent term value d_1 in dependence on phases Poisson's ratios and the shear moduli relation (Fig.1). They provide a qualitative insight into the optimal solution and bridge the gap between the limiting cases of the energy-minimal hole and the rigid inclusion solved previously [1, 2].

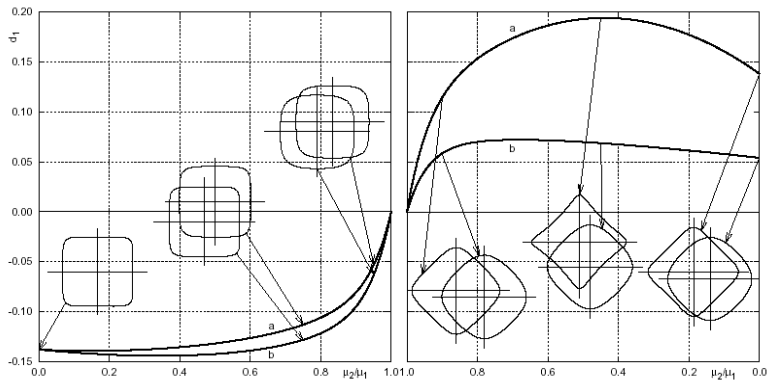

Fig. 1. The admissible intervals for the energy minimizing conformal term d_1 and the corresponding optimal shapes of relatively soft (at the left) and relatively rigid (at the right) inclusion.

Keywords: *Plane elasticity problem, Shape optimization, Extremal elastic structures*.

References:

[1] S.Vigdergauz, "Stress-minimizing hole in elastic plate under remote shear", Journal of Mechanics of Materials and Structures (**1**) (2), 387-406, 2006.
[2] S.Vigdergauz, "Shape optimization of a rigid inclusion in a shear-loaded elastic plane", Journal of Mechanics of Materials and Structures (in press).

Dynamic strength of uranium at high temperatures

E. Zaretsky [1*], B. Herrmann [2], and D. Shvarts [2]

[1] Mechanical Engineering Dept., Ben Gurion University, P.O. Box 653, Beer-Sheva, Israel
[2] Nuclear Research Center - Negev, P.O. Box 9001, Beer-Sheva, Israel
[*] Lecturer: Email: zheka@bgu.ac.il

At room temperature the α-phase of uranium (orthorhombic, 4 atoms per unit cell) is stable up to the pressure of 100 GPa; uranium is the only known actinide which has no phase transitions in this pressure range. Heating of α-uranium up to the temperature of about 680ºC results in its transformation into β-structure (tetragonal, 30 atoms per unit cell, identical to intermetallic σ-phase). Heating above 780ºC results in the appearance of γ-phase (body-centered cubic, 2 atoms per unit cell). The domain of existence of β-uranium is very narrow: being compressed above the α/β/γ triple point (p = 3.5±0.3 GPa) the heated α-uranium transforms, at T ≈ 830ºC, directly into its γ-modification [3]. The cause of the existence of σ-phase of pure element (the σ-phase is well-known for intermetallic compounds, in particular the structure of β-uranium is identical to disordered FeCr σ-phase) in such narrow domain is not clear.

Unalloyed uranium (PU) and uranium-0.78 wt% Ti alloy (UT) were studied in VISAR-monitored planar impact experiments with initial sample temperatures ranged from 27ºC to 860ºC. The recorded waveforms was used for obtaining the stress-strain σ(ε) and deviator stress-strain s(□ε) diagrams, the conventional elastic limit $Y_{0.2}$, and the spall strength of the alloys at different testing temperatures. The strengths $Y_{0.2}$ (Fig.1) of both the materials stay almost constant up to the temperature of α–β transformation, increase strongly in the β-phase domain, and abruptly drop above the temperature of β–γ transformation.

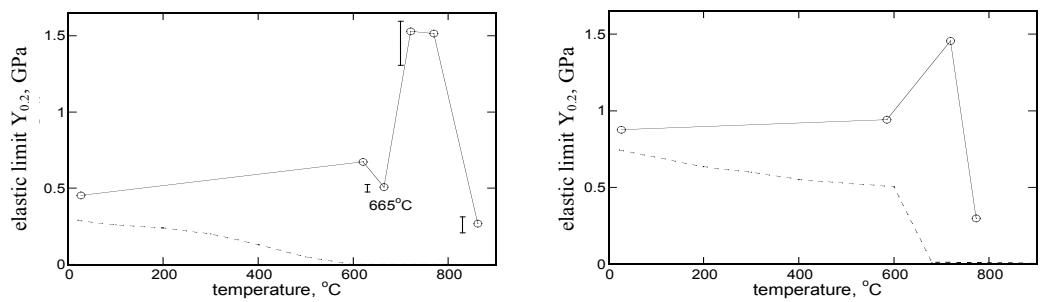

a) b)

Figure1. Temperature dependencies of the dynamic yield strength of PU (a) and UT (b) samples. Solid lines correspond to the strength values obtained in the present work, the dashed lines correspond to the quasi-static literature data. Error bars show uncertainties of the high-temperature properties values.

The temperature dependences of the spall strength of alloys differ from those of the compressive strengths indicating the prevailing role of the void nucleation (over the void growth) in the spallation process. The most striking finding of the work is the existence of β-uranium at pressures some 3 GPa higher than that permitted thermodynamically. The life time and the borders of existence of this non-equilibrium phase are unknown and should be determined in future.

Keywords: *Uranium, phase transitions, dynamic strength.*

Large strain response of uniformly stressed elastoplastic solids under superposed simple shear

E. Chesla* and D. Durban

Faculty of Aerospace Engineering
Technion – Israel Institute of Technology
Haifa 32000, Israel
*Lecturer: Email: maromc@gmail.com

The effect of initial uniform tension (compression) on elastoplastic response of compressible solids, under superposed simple shear, is examined within the framework of finite strain J_2 theories. Exact continuum plasticity equations are derived and solved analytically for the flow, deformation and hypoelastic deformation-type theories. Isotropic hardening is considered with arbitrary strain hardening (softening) characteristics. Specific examples include the Ramberg-Osgood and elastic/linear-hardening materials. Elastic compressibility is accounted for in all models, yet practical relations are given for the deep plastic range with vanishing compressibility. An elegant by-product of the flow theory analysis is that with elastic/perfectly-plastic response we recover Prager`s classical hardening (tanh) rule for superposed shear.

The solution method centers on the effective Mises stress as the independent variable and on quadratures for field variables in flow and hypoelasic models. For the model of deformation theory (which is essentially a Cauchy elastic solid) we obtain algebraic expressions. Initial plastic strain is shown to have an appreciable effect on superposed simple shear behavior, particularly with the deformation theory and its hypoelastic version, due to weakening of instantaneous shear modulus. We provide a detailed comparison among the shear stress-strain curves (based on identical axial stress-strain curves) of the three competing models, with special emphasis on points of instability (maximum shear stress). Also discussed, are the normal stress components needed to sustain simple shear, superposed on axial pre-strain, and thickness changes during shear.

Key results are supported by asymptotic relations along with a sample of numerical illustrations. A few analytical approximations are shown to agree quite well with exact results and contact is made with earlier studies on restricted versions of the problem (e.g. assuming complete incompressibility, or with no initial strain). The implications of the present study to experimental work on plastic stress-strain curves are discussed. Finally, we show how the this analysis can be used to the large strain elastoplastic problem of simple torsion applied to circular (compressible) cylinders with axial pre-stress.

Electroactive polymer composites – coupled electro-mechanical FE analysis

D. Shaine*, L. Tevet-Deree and G. deBotton

Department of Mechanical Engineering
Ben-Gurion University, Beer-Sheva 84105
http://www.bgu.ac.il/~debotton; Email: debotton@bgumail.bgu.ac.il
*Lecturer

This work is concerned with the class of electroactive polymers (EAP), known also as "artificial muscles", due to their respond to electrical simulation with large displacement. These actuator materials provide attractive advantages: they are soft, light-weight, can undergo large deformation, possess fast response time and are resilient. However, wide-spread application has been hindered by their limitations: the need for large electric field, relatively small forces and energy density. It is now recognized that the limitations arise from poor electro-mechanical coupling in typical polymers: this in turn is related to the fact that the typical polymers have a small ratio of dielectric to elastic modulus (flexible polymers have low dielectric modulus while high dielectric moduli polymers are stiff). Recent experimental work (e.g. [1]) shows great promise that this limitation can be overcome by making composites of flexible and high dielectric modulus materials.

There are two main difficulties associated with the characterization of the behavior of Electroactive polymer composites [2]. Both these difficulties are related to the primary advantages of these actuators. The first is associated with the nonlinear coupling between the applied electric fields and the induced mechanical fields. This nonlinearity can result in amplification of the mechanical fields by local concentrations in the electric field. The second difficulty results from the main advantage of these actuators namely the large actuation strains. As a consequence the description of the actuators' behavior must be done within the finite deformation theory of Elasticity.

The goal of this work is to develop a finite element based solver for the combined electro-mechanical analysis of the behaviors of these composite actuators. We present preliminary results demonstrating the ability of the proposed procedure to predict the actuations of these composites due to electrostatic excitations. In the future this finite element technique will be used for optimizing the microstructures of the composites.

Keywords: *Electroactive polymers, Smart materials, Finite deformations, Homogenization, Electrostatic actuation*.

References

[1] Q. M. Zhang, H. Li, M. Poh, F. Xia, Z.-Y. Cheng, H. Xu, and C. Huang. An all-organic composite actuator material with a high dielectric constant. *Nature*, **419**:284–289, 2002.

[2] G. deBotton, L. Tevet-Deree, and E. A. Socolsky. Electroactive heterogeneous polymers: analysis and applications to laminated composites. *Mechanics of Advanced Materials and Structures*, **14**:13–22, 2007. http://dx.doi.org/10.1080/15376490600864372

Experimental investigation of contact area during normal loading-unloading in elastic-plastic spherical contact using direct optical technique.

A. Ovcharenko*, G. Halperin and I. Etsion

Faculty of Mechanical Engineering, Technion - Israel Institute of Technology
Haifa 32000, Israel.

*Lecturer: Email: andreyo@technion.ac.il

The real contact area between a sphere and a flat during loading and unloading process in the elastic-plastic regime of deformations was investigated experimentally. A direct optical technique was used to observe in situ the evolution of the contact area. The experimental results obtained with copper (Cu) and stainless steel (SS) spheres of different diameters that were pressed against a sapphire flat were compared with existing theoretical models in loading and unloading process.

All the experimental contact area results for the entire list of sphere diameters and materials (see Table 1) under the full range of normal loads (P=0.5-190N) are presented and compared in Figure 1 with the theoretical model assuming slip (i.e. frictionless) [1] contact condition. The experimental results of the contact area, A and normal load, P were normalized by A_c and P_c, respectively (where A_c is the critical contact area and P_c is the critical normal load at yield inception, assuming slip contact condition [3]). As can be seen in Figure 1, the theoretical model describes very well the experimental results for the entire range of normal loads. It is clear that proper normalization by the relevant critical values of the contact parameters provides a powerful universal relation between contact area and normal loading for specimens of different diameters and materials.

Figure 2 shows the contact area during unloading of both the copper and stainless steel spheres with their different diameters as shown in Table 1. The results are compared with the theoretical loading-unloading model [2]. The spheres were unloaded from three different values of maximum dimensionless load P_{max}/P_c (see Figure 2). The curve fits for the theoretical results during unloading [2] (dashed lines), and during loading [1] (solid line), are also shown for comparison. As can be seen the model in [2] predicts well the unloading experimental results except for a short range, close to the beginning of the unloading process. As can be seen from the unloading results a proper normalization of the contact parameters by their relevant critical values provides, like in the loading case, a universal similarity relation between the normalized contact area and normal load for the entire specimens population of different diameters and materials.

R_a [nm]	P_c [N]	E [GPa]	ν	Y [MPa]	H [GPa]	D [mm]	Material	Symbol	Case
100	0.43	139	0.33*	345	1.15	5	Copper	▲	1
100	1.73	139	0.33*	345	1.15	10	Copper	■	2
100	4.21	139	0.33*	345	1.15	15	Copper	●	3
50	1.69	200	0.30*	1080	3.76	2.38	Stainless Steel	○	4
50	6.77	200	0.30*	1080	3.76	4.76	Stainless Steel	□	5
5	-	435*	0.27*	2950*	19*	flat	Sapphire	None	

** values obtained from the literature*

Table 1. The mechanical and geometrical properties of copper (Cu) and stainless steel (SS) spherical specimens, and sapphire flat. (D - diameter, H - hardness, Y - yield strength, ν - Poisson's ratio, E - Young's modulus, R_a - roughness average, P_c - critical normal load at plastic yield inception in slip respectively [3]).

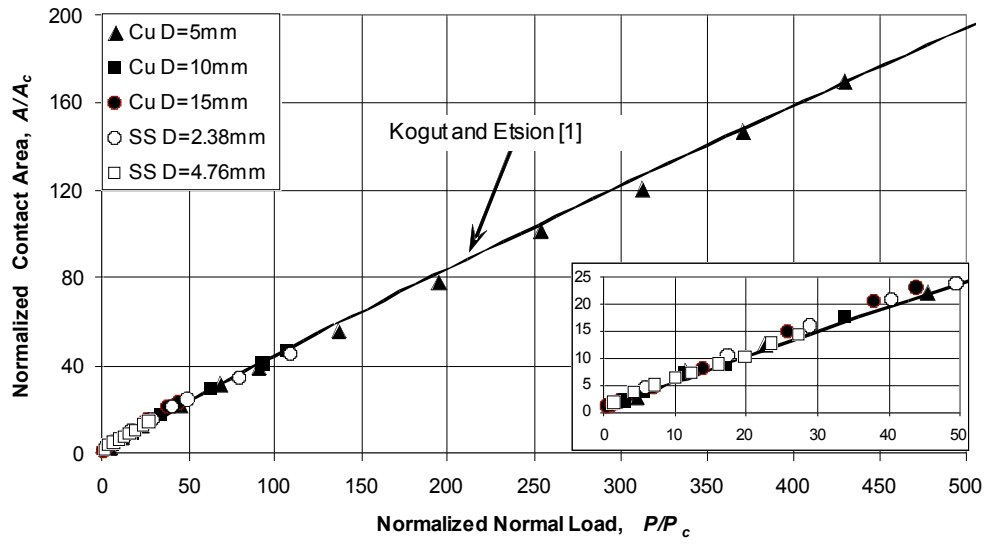

Fig. 1. Comparison of normalized contact area vs. normalized normal load under assumed slip contact conditions.

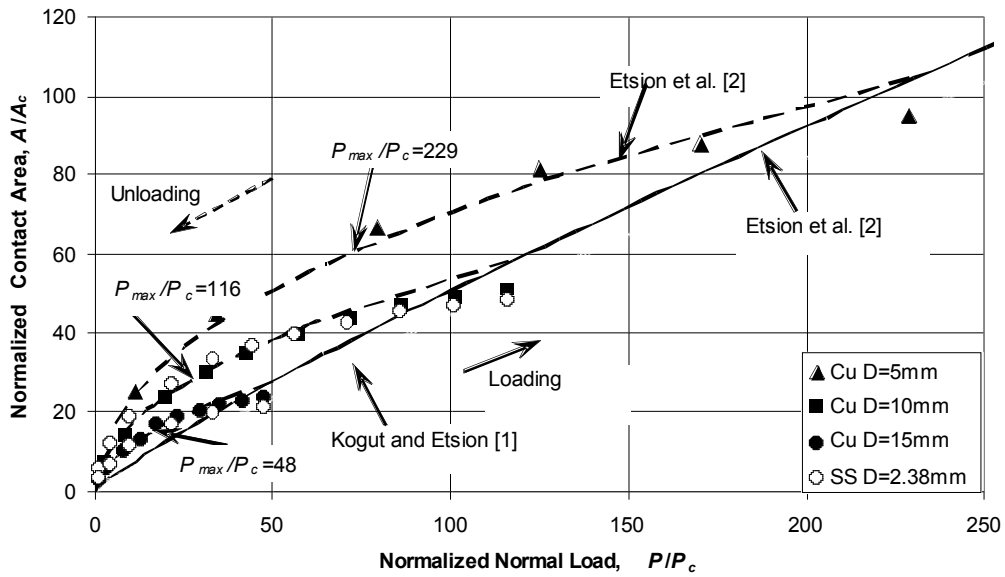

Fig. 2. Comparison of the experimental and theoretical contact area vs. normal load during unloading. The results are normalized by their corresponding critical values at yield inception assuming slip contact condition.

Keywords: *elastic-plastic spherical contact, loading-unloading, contact area.*

References

[1] L. Kogut and I. Etsion, "Elastic-Plastic contact analysis of a sphere and a rigid flat", ASME J. Appl. Mech. 69, 657-662 (2002).

[2] Etsion, Y. Kligerman and Y. Kadin, "Unloading of an elastic-plastic loaded spherical contact", Int. Journal of Solids and Structures 42, 3716-3729 (2005).

[3] V. Brizmer, Y. Kligerman and I. Etsion, "The Effect of conditions and material properties on the elasticity terminus of a spherical contact", Int. J. of Solids and Structures 43, 5736-5749 (2006).

Elastic-Plastic Spherical Contact under Combined Normal and Tangential Loading

V. Brizmer*, Y. Kligerman, I. Etsion

Faculty of Mechanical Engineering Technion - Israel Institute of Technology
Haifa, 32000, Israel
*Lecturer: Email: brizmer@technion.ac.il

The behavior of an elastic-plastic contact of a deformable sphere and a rigid flat under combined normal and tangential loading with full stick contact condition is investigated theoretically. This allows static friction modeling under highly adhesive conditions. Combined loading begins with a normal preload that produces an initial contact area and causes elastic or elastic-plastic deformations in the contact zone. The full stick contact condition leads to a junction between the contacting bodies which can bear tangential loading. On the second stage of the loading process, the tangential load is being applied gradually, while the normal load remains constant. The maximum tangential load that can be supported by the junction prior to sliding inception is determined as the static friction. The effect of normal load on this static friction is investigated. The evolution of the contact area during the tangential loading revealed an essential "junction growth" mainly just before sliding inception.

Fig. 1 presents a deformable sphere of a radius R in contact with a rigid flat under combined normal and tangential loading. The bold and thin dashed lines show the contours of the sphere before and after applying the normal load, P, respectively, while the solid lines show the final contours of the contacting bodies after applying the tangential load, Q. The normal load produces an initial normal interference, ω_0, and an initial circular contact area of a diameter d_0. The succeeding application of a tangential load causes an increase of these initial interference and initial contact area. The final interference and diameter of the contact area are denoted as ω and d, respectively.

The behavior of elastic-plastic spherical contact under combined normal and tangential loading was investigated over a wide range of dimensionless normal loads from elastic to deep elastic-plastic contact: $0.5 \le P^* \le 200$, where P^* is P / L_c and L_c is the critical normal load in stick, at yielding inception. A Poisson's ratio 0.3, typical for ductile metals, was selected in the present analysis along with a typical value $E/Y_0 = 1000$ for the Young's modulus over the virgin yield strength ratio.

Fig. 2 shows the numerical results for the dimensionless maximum tangential load, Q_{max}/L_c, and the static friction coefficient, Q_{max}/P, just before sliding inception, as a function of the dimensionless normal load, P^*. As can be seen from Fig. 2, the static friction coefficient decreases sharply with increasing normal load up to about $P^* = 20$. From there on the rate of decrease in the friction coefficient diminishes, and at $P^* = 200$ it approaches a constant value of about 0.27.

Experimental results for the contact of smooth copper balls (with Poisson's ratio of 0.33) are also shown in Fig. 2 for Q_{max}/P (triangles) and Q_{max}/L_c (circles). Good agreement between the experimental and numerical results is found except for small normal loads ($P^* < 10$), where the model overestimates the experimental results.

It was found that the tangential loading leads to a slight increase in the initial interference (of about 5%) and to a considerable increase in the contact area (junction growth).

Keywords
Elastic-plastic contact, Static friction, junction growth.

Reference

[1] Brizmer, V., Kligerman, Y., and Etsion, I., 2006, "Elastic-Plastic Spherical Contact under Combined Normal and Tangential Loading in Full Stick", *Tribology Letters*, in press.

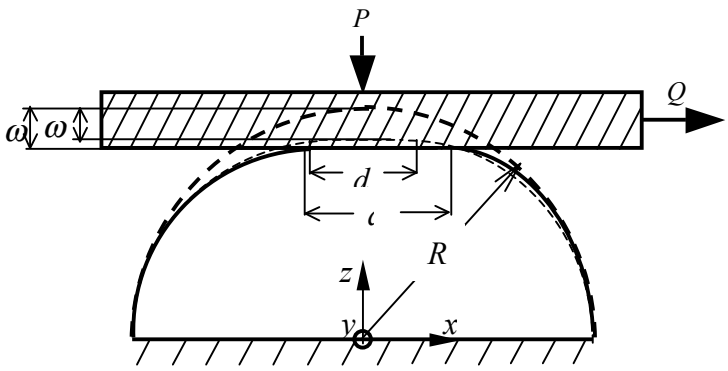

Fig. 1. Model of a deformable sphere in contact with a rigid flat under combined loading.

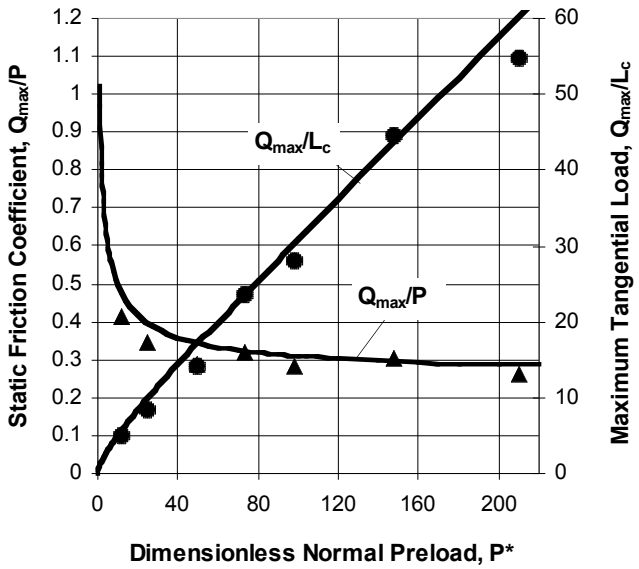

Fig. 2. The dimensionless maximum tangential load, Q_{max}/L_c*, and the static friction coefficient,* Q_{max}/P*, vs. the dimensionless normal load,* P^**.*

Yielding inception of adhesive micro-contact

Y. Kadin*, Y. Kligerman and I. Etsion

Shamban Tribology Laboratory
Faculty of Mechanical Engineering, Technion - Israel Institute of Technology
Haifa 32000, Israel.
*Lecturer: Email: kadin@tx.technion.ac.il

The interaction between deformable solids resulting from physical attractive (Wan der Waals) and repulsive (Born) forces has become an important subject, partly because it can contribute to a better understanding of surface phenomenon (e.g. adhesion and friction) and partly because of its relevance to the contact mechanic of the AFM probe. An impressive number of theoretical studies on elastically deformed bodies have been published; however, a complete investigation of the elasticity terminus condition is still missing.

The main goal of the current research is a quantitative prediction of the yielding inception which may be initiated by adhesive traction alone, acting between approaching spherical micro-bodies. The contact of two elastic spheres can be analyzed by considering the simpler equivalent problem of a sphere with a combined elastic modulus, and an equivalent radius, in contact with a flat rigid surface. The adhesive traction acts on the sphere's surface and its distribution is given by the Lennard-Jones potential as the function of the local gap distribution between the sphere and the flat rigid surface. The calculation of the local gap distribution takes into account the flexibility of the sphere. When the radius of a sphere is much larger than the radius of the contact region, the distribution of the local vertical displacement, of the sphere boundary may be calculated by an integration of the Boussinesq solution. Thus, the local gap distribution depends on the surface traction and vise versa. The desired solution of this problem corresponds to the local gap distribution which provides equilibrium between external adhesive and internal elastic forces. The solution technique is based on the fixed point iteration scheme, which also provides adhesive traction acting on the surface of the sphere and stress field within it.

One of the difficulties to define an elastic limit of micro-contacts is the fact that the strength for small material volumes is much higher than the macroscopic one. This is because the structure of micro-volume has a low probability of imperfections and hence it is close to the ideal mono-crystal. The yield strength of such a small-scale structures approaches its theoretical value, which is the upper bound for all experimentally measured strengths and may be derived from the elastic shear modulus.

The comparison of the equivalent von Mises stress even to the theoretical strength reveals that the adhesive traction alone may cause yielding inception.

Keywords: *Adhesion, Micro-strength*.

Relaxation and pure creep under new paradigm

I. Blechman

Researcher at Technion
Email: isblech@techunix.technion.ac.il

The old paradigm on compliance proposed that creep and relaxation are mutual processes of the same origin, creep being an elasto-plasto-visco process with a reversible part not restricted by time and ending by failure, represented by Kelvin-Maxwell models. It is found now ineffective.

According to a New Paradigm relaxation is an irreversible intrinsic process of stress loss limited in its value and duration. It belongs to the class of exo-processes. Creep is not the opposite of relaxation, since it is combined of two processes: relaxation under constant load and microcracking due to local strains in creeping components against non-creeping parts.

There is a group of **exhausting (exo) processes**, where **a change** in a given feature of a solid *takes finite time* and is monotonic. Its function has the following features: it is monotonic; its function Z_t reaches the limiting value Z_f in finite time – $\tilde{t}_f$. At its beginning Z = 0 and dZ = ∞, at its end dZ = 0. Its differential equation has the form

$$dZ = \square\, c \left(\frac{\tilde{t}_f - \tilde{t}}{Z_t}\right)^{N-1} dt \quad .$$

Its analytical solution is $Z = Z_f \mathcal{B}_t$ where the time-operator (exo-timer) $\mathcal{B}_t$ is

$$\mathcal{B}_t = \left[1 - \left(1 - \frac{\tilde{t}}{\tilde{t}_f}\right)^N\right]^{1/N} \quad .$$

<u>The loss of stresses</u> – σ_x under **relaxation**, called <u>pliancy</u>, has the pattern of an exo-process and the same equation: $\sigma_x = \sigma_{xf}\, \mathcal{B}_t$, σ_{xf} = final stress loss. The equation of stress decrease under relaxation is $\sigma_x = \sigma_{in}\, \mathcal{R}_t$, where $\mathcal{R}_t = (1\square\ \lambda\mathcal{B}_t)$, is the exo-operator of relaxation. It comprises *three material parameters*: the **<u>potential</u>** of complete relaxation: $\boldsymbol{\lambda} = \sigma_{xf}/\sigma_{in}$, (where σ_{in} = initial stress), the **duration of complete relaxation** – $\tilde{\mathbf{t}}_f$ and the exponent – **N**, reflecting the process rate. For structural concrete they are: λ = 0.40, $\tilde{\mathbf{t}}_f$ = 35 days, N = 4, independent of the strains and stresses. The equation of relaxation accords well with the data, especially of *the first seconds and minutes* of rapid drop in the stress, the well known obstacle in existing models.

Pure creep of concrete is defined as a manifestation of relaxation only, without microcracking. Its equation $\varepsilon_c = \varepsilon_{in}\, C_t$, includes the constitutive operator of plain creep $C_t = \lambda\mathcal{B}_t/(1-\lambda\, \mathcal{B}_t)$. The ratio – ρ of pliancy in creep vs. relaxation is: $\rho = 1/(1-\lambda)$. For λ = 0.4, ρ = 1.67.

The exo-description of relaxation and pure creep does not belong to the realm of rheology. It presents a unique state of stress decrease under any load. But in real creep, even under modest stresses, <u>c-microcracks</u> appear, caused by strain gradients between creeping components against non-creeping particles. Microcracking, reducing the integrity of concrete, bring on ”high creep”, with its particular features and its own models.

A Numerical Model for Evaluating the Residual Stress Field in an Autofrettaged Spherical Pressure Vessel Incorporating the Bauschinger Effect

M. Perl[1*] and J. Perry[1]

Pearlstone Center for Aeronautical Engineering Studies
Department of Mechanical Engineering
Ben-Gurion University of the Negev
Beer-Sheva 84105, Israel
*Lecturer: Email: merpr01@bgumail.bgu.ac.il

Abstract

Pressure vessels, mostly cylindrical, are widely used in many industries. However, due to their optimal specific strength (strength/weight) and their ease of packaging, spherical pressure vessels are commonly used for example as: propellant/oxidizer/pneumatic tanks on spacecrafts and aircrafts, gas tanks on LNG (liquefied natural gas) carriers, pressurized storage tanks for chemical substances, cookers for the food industry, and as metal or concrete containment structures in nuclear plants. Furthermore, whenever ***extremely high pressure*** occurs, such as in high explosion containment tanks or in the apparatus used to manufacture artificial diamonds, spherical pressure vessels are the only feasible solution.

In order to further increase the load capacity of such pressure vessels as well as to prolong their fatigue life, a favorable compressive residual stress field is introduced to the inner portion of the vessel's wall by the autofrettage process.

Although there are many studies that investigated the autofrettage problem for cylindrical vessels, only a few solutions were recently proposed for spherical vessels. The purpose of this research is to extend the existing experimental-numerical model of the autofrettaged cylinder [1], in order to offer a more realistic solution for the residual stress field in an autofrettaged spherical pressure vessel, incorporating the Bauschinger effect.

Two main processes are used to autofrettage cylindrical pressure vessels: hydrostatic autofrettage and the autofrettage. The hydrostatic autofrettage is modeled as an axisymetric, two-dimensional problem solved in terms of the radial displacement solely, while the three-dimensional swage autofrettage is solved in terms of the radial and the axial displacements. Due to it symmetries, spherical autofrettage is to be treated as a two-dimensional problem and solved in terms of the radial displacement only, as the case is for hydrostatic autofrettage in a cylinder.

The two-dimensional mathematical model is based on the idea of solving the elastic-plastic autofrettage problem using the form of the elastic solution [1]. The elastic strains are replaced in Hooke's law by the difference between the total and plastic strains. Substituting these new Hooke's equations into the equilibrium equation and using the strain-displacement relations, yields a differential equation of the radial displacements in terms of plastic strains:

$$\frac{d^2u}{dr^2}+\frac{2}{r}\frac{du}{dr}-\frac{2}{r^2}u=F(\varepsilon_r^p;\varepsilon_\theta^p)$$

The plastic strains are calculated based on the Prandtl-Reuss flow rule and the universal stress-strain curve. The differential equation is solved by the explicit finite difference method, while the wall of the spherical shell, of inner radius a and outer radius b, is divided into N-equal parts of thickness $\Delta r=(b-a)/N$.

The unique material model proposed by Perry and Perl [1], which was used to determine the autofrettage residual stress field in a cylindrical pressure vessel, is applied to the spherical pressure vessel, herein analyzed. The elastic-plastic material behavior during the loading (pressurization) and unloading (depressurization) phases is simulated by a four segments stress-strain curve. During the loading the material behaves elastically up to the yield point, beyond which the behavior is modeled by the universal stress-strain curve. This curve is represented by the plastic portion of a uniaxial tensile test curve. Prior to unloading, the current Young's modulus and the

[1] Aaron Fish Professor of Mechanical Engineering-Fracture Mechanics and Graduate student, respectively.

compressive yield stress are evaluated taking in to account the Bauschinger effect. The universal tensile curve of the loading stage is replaced by the compressive one, represented by the average of the all compressive uniaxial stress-strain curves, beyond their respective reduced yield points. To find the exact yield points in tension and compression, a unique definition for the zero offset yield point is used.

The existing 2-D computer program developed for hydrostatic cylindrical autofrettage calculations was modified to accommodate the spherical autofrettage case, and the appropriate residual stresses were evaluated. The residual stresses are compared with existing solutions for spherical autofrettage and are found in very good agreement, as can be seen from the following figure, which compares the present results with those of Parker and Huang [2].

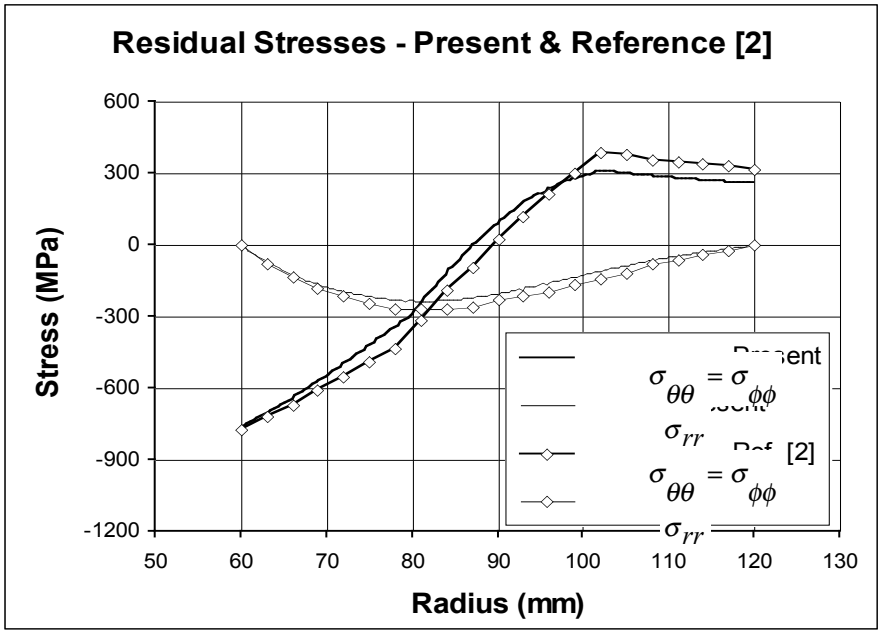

References

[1] Perl, M., Perry, J., 2005, “An Experimental-Numerical Determination of the Three Dimensional Autofrettage Residual Stress Field Incorporating Bauschinger Effect,” Trans. of the ASME, Journal of Pressure Vessel Technology, 128, pp. 173-178.

[2] Parker, A. P., Huang, X., 2006, "Autofrettage and Re-autofrettage of a Spherical Pressure Vessel," Trans. of the ASME, Journal of Pressure Vessel Technology, in press.

Open mechanics problems in Biomechanics and Robotics

A. Wolf

Head, Biorobotics and Biomechanics Lab (B.R.M.L)
Technion Israel Institute of Technology
Faculty of Mechanical Engineering
Tel: +972-4-8292087; Fax:+972-4-8295711
Web: http://meeng.technion.ac.il/Personnel/Faculty/Wolf/

"The only true wisdom is in knowing you know nothing."
"The wise speak only of what they know." …(Socrates)

This talk is about what we know that we do not know and would like to know more.

As researchers and engineers we often develop and invent mechanisms that work well however when it comes to modeling their behavior there is a gap between what we know and what we do not know. Moreover, we are constantly introduced to new research areas which involve new technologies, materials and structures never dealt before. Consequentially existing classical mechanical models are often not valid anymore, these models need to be adjusted or modified to better describe and deal with the evolving technologies.

Biomechanics is an example for a relatively new research area where existing computational mechanical models are often not sufficient to describe the behavior of a biological tissue. For example, typical joint movement during normal function involves a complex set of coupled translation and rotation. Knowledge of the in vivo movement of the joint is important for understanding normal function as well as addressing clinical problem and pathologies. The most frequently used method for measuring joint movement involves placing optical markers on the skin surface of the segment being analyzed. These markers are tracked by a set of cameras which then extract the skeletal motion. However, the estimation of the skeletal motion obtained from marker-based motion capture systems is known to be affected by significant bias caused by skin movement artifact, which affects later biomechanics calculation (e.g. forces, torques, deformations etc..). Human skin is a complex tissue consisting of several distinct layers. Each layer consists of various components with a specific structure. Mechanical behavior of the human skin is comple, it shows a non-linear stress-strain relationship, behaves time-dependent, in compressible, anisotropic and inhomogeneous. Mechanical modeling of the human skin is an example for a new research area where better mechanical models are required.

Still in the Biomechanics area. When studying the behavior and function of the large joints, i.e. knee, hip, shoulder, elbow, it is evident that the motion is mainly constraint by the soft tissues which are connecting the bones, e.g. ligaments, cartilage. Ligaments, for example are soft collagenous tissues contains collagen fibrils. As with all biological tissues, ligaments have a hierarchical structure that affects their mechanical behavior. In addition, ligaments can adapt to changes in their mechanical environment due to injury, disease or exercise. Precise modeling of the mechanical properties and behavior of these tissues enable better understanding of the mechanical contribution of each of the ligaments and the overall kinematic description of the joint motion. This understanding can lead to better implant design, artificial limbs design and more tailored and patient specific operational techniques.

Robotics is a relatively new area of engineering. One of the major constraint that roboticists have when designing a new robotic system is availability of proper actuation. There is usually a tradeoff between physical size of the motor, its power, and workspace, i.e. how much it can move. For that reason we try to introduce a new concept of *Bi-material* bellows which are composed of two different materials. The two materials have two different *shear modulus*: one has high elasticity and the other low. By applying pressure inside the bellows each of the material tends to deform. Yet due to the boundary constraints, i.e. both half bellows have to move together, the high shear modulus material will undergo a larger strain than the one with the low shear modulus causing the bellow to bend (like a bimetallic strip). With this kind of idea we were able to achieve a 180 degree turn of a 10mm in diameter, 10 cm long silicon based bi-bellow. These results seems to be very promising however, this new actuation method would be almost worthless without a proper kinematic model that takes into account all the control parameters of the device and provides a mechanical modeling of the device deflection under controlled pressure. Needless to say that this is a very challenging task given the high deformations and non linearity.

To conclude; in this talk I will present several areas of research where current mechanical models are not up-to-date and not general enough do describe phenomenon. In such cases there is a need for better and new mechanical modeling that would enable to bridge the gap between what we know and what we know that we do not know.

Dynamics of Cell Orientation

R. De*, A. Zemel, and S.A.Safran

Department of Materials and Interfaces,
Weizmann Institute of Science, Rehovot 76100, Israel
*Lecturer: Email: rumide@wisemail.weizmann.ac.il

Many physiological processes, such as bone and muscle growth, wound healing, and angiogenesis depend on the response of cells to mechanical forces; these can be generated either by the contractile activity of the cell or by external stresses. Understanding the response of cells embedded in gel matrices to mechanical loading is important not only for basic biological science but also for the rational design of artificial tissues. In recent years, it has been established that cells can actively sense the mechanical properties of their environment and respond in various ways [1]. By pulling on their environment, cells actively sense rigidity gradients, boundaries and applied strains [2]. Cells respond to these signals by actively adjusting their contractile activity. When plated on rigid elastic substrate many cell types show increased spreading and better developed stress fibers and focal adhesions (FA) compared with floating (and elastically non-resistant) substrates [3]. Another ubiquitous and puzzling experimental observation is that cells respond differently when the matrix is subjected to static strain compared with dynamically varying strain. For static strain, cells align parallel to the direction of applied strain [4] while for cyclic strain, cells align nearly perpendicular to the direction of applied strain [5].

Using a simple theoretical model that includes the forces due to both the mechanosensitive nature of cells and the elastic response of the matrix, we predict the dynamics and orientation of cells in both the absence and presence of applied stresses. Our model, that contains only two dimensionless parameters that can be measured by force experiments, predicts many features observed in measurements of cellular forces and orientation including the increase with time in the forces generated by cells in the absence of applied stress and the consequent decrease of the force in the presence of quasi-static stresses. We also explain the puzzling observation of cells that align parallel to the direction of applied force for quasi-static stresses and the nearly perpendicular alignment of these cells for dynamically varying forces.

References

[1] Harris A.K., Wild P. and Stopak D, Science, vol. 208, pp 177-179 (1980).
[2] Engler A. J., Sen S., Sweeney H. L. and Discher D. Cell, Vol. 126, pp677-689 (2006).
[3] Grinnell F., trends in Cell Biology, vol. 10, pp 362-365 (2000).
[4] Eastwood M., Mudera V. C., McGrouther D.A., and Brown R.A., Cell Motil. Cytoskeleton, vol 40, pp 13-21 (1998).
[5] Wang J. H-C.,Goldschmidt-Clermont P., and Wille J., J. Biomech., vol 34, pp 1563-1572 (2001).

A generalized 3-d brick Cosserat point element for nonlinear elasticity: Comparison with other element formulations

M. Jabareen* and M. B. Rubin

Faculty of Mechanical Engineering, Technion - Israel Institute of Technology
32000 Haifa, Israel.
*Lecturer: Email: cvjmah@tx.technion.ac.il

Introduction

In spite of many years of finite element technological development there still appears to be a need for a robust user friendly element for nonlinear elasticity. Specifically, the numerical solution of challenging real problems still needs an expert user who can identify areas of the mesh which might be adversely affected by artificial numerical locking due to poor aspect ratios, near incompressibility or hourglassing. Within the context of standard finite element procedures attempts have been made to develop an element based on one-point integration and stabilization methods for inhomogeneous modes of deformation. Moreover, for a user friendly element the stabilization procedures should need no user intervention.

Recently, Nadler and Rubin [1] developed a 3-D eight noded brick element based on the theory of a Cosserat point. In contrast with standard finite element procedures the Cosserat approach treats the element as a structure and proposes as strain energy function for homogeneous and inhomogeneous deformations. The constitutive response needs no integration through the element region and the functional form of the strain energy has been restricted so that a nonlinear form of the patch test is automatically satisfied for arbitrary reference shapes of the element.

In the original formulation [1], the part Ψ of the strain energy function that characterizes the response to inhomogeneous deformations was taken to be a quadratic function of inhomogeneous strain measures and the coefficients were determined by matching exact linear solutions of bending, torsion and higher-order houglassing for a rectangular parallelepiped. This Cosserat point element has been shown [2,3] to respond well for nonlinear elastic problems which typically exhibit locking and hourglassing. However, in [2] it was shown that the response of this element for irregular shaped elements could be improved. Motivated by this conclusion, Jabareen and Rubin [4] developed a generalized 3-D Cosserat brick element which responds well for irregular shaped elements. Specifically, in [4] the strain energy Ψ was generalized to include dependence on the reference geometry of the element and additional bending solutions for non-rectangular parallelepiped elements were considered to determine the functional dependence of the coefficients in Ψ on the reference geometry. The resulting generalized Cosserat point brick element was shown to be accurate and robust for irregular shaped elements

Discussion and summary

Figure 1 shows the predictions of the Cosserat point element and those of an enhanced strain element in the computer code FEAP for the large deformation Cook's membrane considered in [4]. Specifically, it can be seen that the FEAP element predicts unphysical hourglassing at the inner edge of the membrane.

A number of example problems, which include small and large deformations and irregular shaped elements, have been considered to compare the predictions of the generalized 3-D Cosserat point brick element with other element formulations in the computer codes ABAQUS, ADINA, ANSYS and FEAP. It has been shown that the Cosserat point element is also applicable to thin structures, its is as accurate as elements based on the enhanced strain and incompatible mode methods and is as robust as the full integration element. Moreover, the Cosserat point element does not suffer from hourglass instabilities that are observed in the enhanced strain and incompatible mode elements in problems with combined high compression and inhomogeneous deformation. The Cosserat point element is hyperelastic, needs no integration through the element region, no user specified hourglass parameters and can be used for plates and shells since it does not exhibit locking for large aspect

ratios or nearly incompressible material response. Consequently, the generalized Cosserat point brick element is truly a user friendly element that can be used with confidence for the complete range of challenging real problems in finite elasticity.

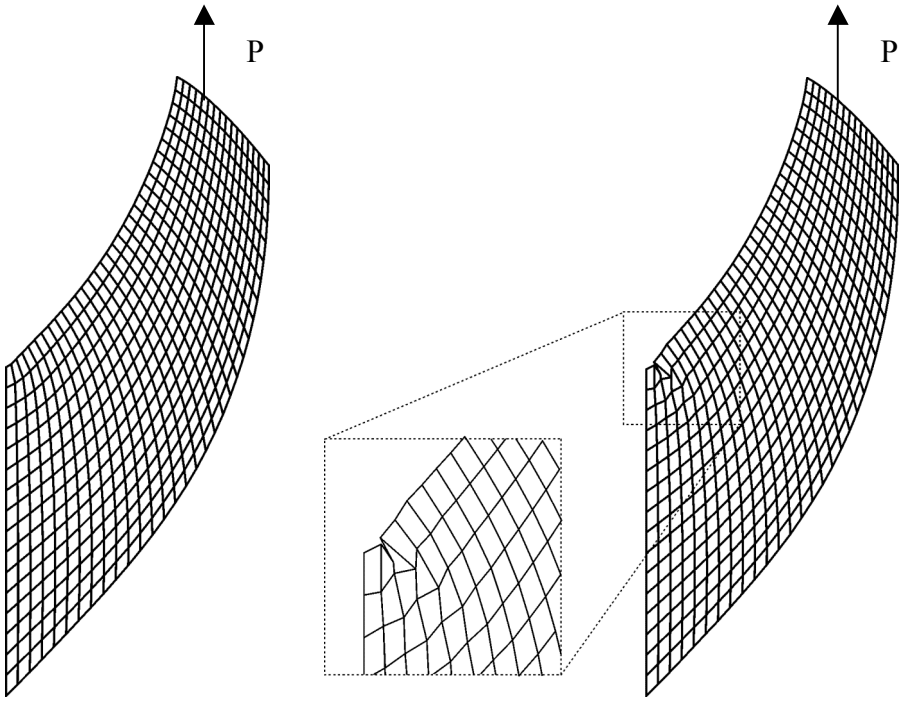

(a) Generalized Cosserat (b) FEAP

Fig. 1. Cook's membrane. Nonlinear deformations for the mesh {32×16×1}, showing physical deformations predicted by the generalized Cosserat element and unphysical hourglassing predicted by FEAP-3 for P = 3.2 kN.

References:

[1] Nadler, B. and Rubin, M.B. (2003): "A new 3-D finite element for nonlinear elasticity using the theory of a Cosserat point", *Int. J. Solids and Structures* Vol. 40, pp. 4585-4614.

[2] Loehnert, S., Boerner, E.F.I., Rubin, M.B. and Wriggers, P. (2005): "Response of a nonlinear elastic general Cosserat brick element in simulations typically exhibiting locking and hourglassing". *Computational Mechanics* Vol. 36, pp. 255-265.

[3] Jabareen, M. and Rubin, M.B. (2006): "Hyperelasticity and physical shear buckling of a block predicted by the CPE compared with inelasticity and hourglassing predicted by other element formulations". To appear in *Computational Mechanics.*

[4] Jabareen, M. and Rubin, M.B. (2006): "A generalized 3-D brick Cosserat point element for irregular shaped elements". Submitted for publication in *Computational Mechanics*.